

# A Novel Tree Model-based DNN to Achieve a High-Resolution DOA Estimation via Massive MIMO Receive Array

Yifan LI<sup>1</sup>, Feng SHU<sup>2</sup>, Yaoliang SONG<sup>1</sup>, Jiangzhou WANG<sup>3</sup>

<sup>1</sup> School of Electronic and Optical Engineering, Nanjing University of Science and Technology, Nanjing 210094, China

<sup>2</sup> School of Information and Communication Engineering, Hainan University, Haikou 570228, China

<sup>3</sup> School of Engineering, University of Kent, Canterbury CT2 7NT, United Kingdom

liyifan97@foxmail.com

Submitted June 16, 2024 / Accepted August 15, 2024 / Online first September 30, 2024

**Abstract.** To satisfy the high-resolution requirements of direction-of-arrival (DOA) estimation, conventional deep neural network (DNN)-based methods using grid idea need to significantly increase the number of output classifications and also produce a huge high model complexity. To address this problem, a multi-level tree-based DNN model (TDNN) is proposed as an alternative, where each level takes small-scale multi-layer neural networks (MLNNs) as nodes to divide the target angular interval into multiple sub-intervals, and each output class is associated to a MLNN at the next level. Then the number of MLNNs is gradually increasing from the first level to the last level, and so increasing the depth of tree will dramatically raise the number of output classes to improve the estimation accuracy. More importantly, this network is extended to make a multi-emitter DOA estimation. Simulation results show that the proposed TDNN performs much better than conventional DNN and root multiple signal classification algorithm (root-MUSIC) at extremely low signal-to-noise ratio (SNR) with massive multiple input multiple output (MIMO) receive array, and can achieve Cramer-Rao lower bound (CRLB). Additionally, in the multi-emitter scenario, the proposed Q-TDNN has also made a substantial performance enhancement over DNN and Root-MUSIC, and this gain grows as the number of emitters increases.

## Keywords

DOA estimation, DNN, massive MIMO, multi-label learning

## 1. Introduction

Direction-of-arrival (DOA) estimation has been a widely studied topic in wireless communications, array signal processing, radar and sonar for few decades [1–4]. One of the most important directions is how to improve

the estimation precision, especially in poor signal conditions such as low signal to noise ratio (SNR) and low number of snapshots. In recent years, with the development of massive multiple input multiple output (MIMO) technology, some works considered massive receive arrays for improving the spatial resolution and DOA estimation precision [5–7]. However, the massive MIMO arrays with fully-digital structures can result in the significantly increasing of hardware costs, so the hybrid analog and digital (HAD) structures are preferred in recent years [8], [9].

Nowadays, deep learning (DL) techniques have been introduced into DOA estimation, by matching the principles of DOA estimation with the frameworks of supervised learning. Many high-precision methods can be trained via prior DOA data for various scenarios. Work [10] proposed a deep neural network (DNN) structure for super-resolution channel estimation and DOA estimation based on massive MIMO system. A DNN-based method was also proposed for hybrid massive MIMO systems with uniform circular arrays (UCA) in [11]. Convolution neural network (CNN) is another technique widely considered in DOA estimation, like [12] designed a CNN-based method for improving precision in low SNR, and [13] introduced CNN for DOA estimation with sparse prior. Overall, traditional DL-based DOA estimation methods usually employ a flat single-level network structure [14], [15], each output class corresponding to a specific direction and the estimation results can only be generated from these fixed directions. So they have high-resolution for on-grid DOAs and have accuracy lower bounds much higher than Cramer-Rao lower bound (CRLB) for off-grid DOAs [16]. Then conventional single-network models have to increase the number of output classes to improve spatial resolution and also cause the serious increase of model complexity. so they can't achieve the best accuracy when estimating off-grid angles for the grid mismatch effect. The easiest way for overcoming this effect is increasing the output classes of networks to improve the angular resolution, while this operation can cause the decrease of model accuracy.

Therefore, a tree-model based DNN (TDNN) scheme is proposed in this work for solving this problem and improving DOA estimation accuracy.

In addition, how to apply the multi-label learning algorithms for the multi-emitter cases is also a key problem in DOA estimation with DL techniques. Traditional multi-label learning algorithms like binary relevance, label ranking, multi-class classification can transform complex multi-labeling problems into more accessible single-labeling problems, and methods with another idea are working to apply existing machine learning algorithms to multi-label learning, such as multi-label K-nearest neighbor (ML-KNN), multi-label decision tree (ML-DT), rank support vector machine (Rank-SVM), etc. [17]. Then based on the ideas of multi-labeling learning, reference [18] applied the DNN model for DOA estimation of multi targets, but the DOA estimation accuracy will significantly decrease with the growth of source number and method to improve the resolution of multi-emitter DOA estimation will be studied in this work.

In order to address the problems of DL-based DOA estimation, a novel DNN architecture called TDNN is studied in this work and a high-resolution TDNN-based multi-emitter estimator is also proposed. Paper [19] considered a scenario that the passive receive array with hybrid structure and worked on solving the phase ambiguity problem in DOA estimation caused by this structure, which is totally different from the problem of DOA estimation via fully-digital receive array discussed in this paper. Then the main contributions of this work are summarized as follows:

1. To improve the DOA estimation accuracy and decrease the model complexity of single network, a multi-level tree-based DNN model is proposed, where each level uses small-scale MLNNs as nodes to divide the angular interval into sub-intervals, and each output class is associated to a MLNN at the next level. Then the number of output classes is gradually increasing from the first level to the last level, so TDNN can significantly improve the estimation accuracy by augmenting the depth of the tree instead of enlarging the scale of single network. Simulation results show the proposed TDNN has much better performance than conventional DNN and root-MUSIC at low SNR, and can achieve CRLB as well.
2. To address the multi-emitter DOA measurement, TDNN is also extended to multi-emitter scenarios. Combining  $Q$  parallel TDNNs forms the  $Q$ -TDNN method, which can estimate  $Q$  different DOAs with same input. The simulation results show that the proposed  $Q$ -TDNN has made a substantial performance enhancement over conventional methods with much lower computation complexity, and this gain grows as the number of emitters increases.

The remainder of this paper is organized as follows. Section 2 introduces the system model. Section 3 proposes the tree-based DNN model for DOA estimation, and the

proposed model is extended to multi-emitter scenarios in Sec. 4. Finally, simulation results and conclusions are given in Secs. 5 and 6 respectively.

*Notations:* Matrices, vectors and scalars are represented by letters of bold upper case, bold lower case, and lower case, respectively. Signs  $(\cdot)^T$ ,  $(\cdot)^*$  and  $(\cdot)^H$  denote transpose, conjugate and conjugate transpose.  $\|\cdot\|$  is the Euclidean norm.  $\text{Re}(\cdot)$  and  $\text{Im}(\cdot)$  stand for the real part and imaginary part of a complex number.

## 2. System Model

As shown in Fig. 1, we consider  $Q$  far-field narrow-band signals impinge onto an  $M$ -element uniform linear array (ULA). The  $q$ -th signal is expressed as  $s_q(t)e^{j2\pi f_c t}$ , where  $s_q(t)$  is the baseband signal and  $f_c$  is the carrier frequency. The received signal at the  $m$ -th antenna is expressed as [8]

$$y_m(t) = \sum_{q=1}^Q s_q(t)e^{j2\pi f_c(t-\tau_{q,m})} + v_m(t) \tag{1}$$

where the narrowband assumption  $s(t) = s(t - \tau_{q,m})$  is exploited, and  $\tau_{q,m}$  denotes the propagation delay of the  $q$ -th signal to the  $m$ -th antenna, which is defined as

$$\tau_{q,m} = \tau_0 - \frac{(m-1)d \sin \theta_q}{c} \tag{2}$$

where  $\tau_0$  is the propagation delay from the signal to a reference point of the array,  $d$  and  $c$  represent the antenna spacing and light speed respectively. Then by combining the received signals of all the antennas we can get

$$\begin{aligned} \mathbf{y}(t) &= e^{j2\pi f_c t} \sum_{q=1}^Q \mathbf{a}(\theta_q) s_q(t) + \mathbf{v}(t) \\ &= e^{j2\pi f_c t} \mathbf{A}(\boldsymbol{\theta}) \mathbf{s}(t) + \mathbf{v}(t). \end{aligned} \tag{3}$$

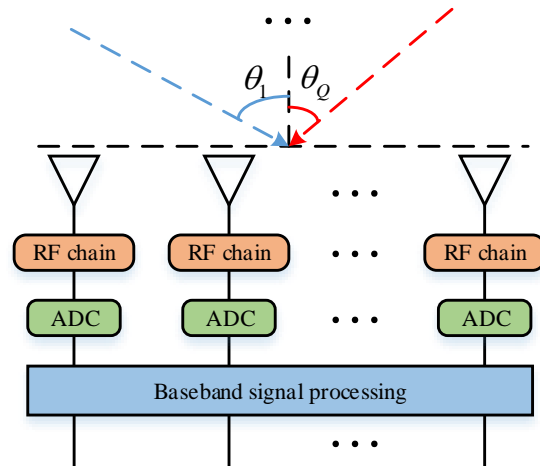


Fig. 1. System model.

After the down conversion and ADC operation, the received baseband signal is given as

$$\mathbf{y}(t) = \sum_{q=1}^Q \mathbf{a}(\theta_q) s_q(t) + \mathbf{v}(t) = \mathbf{A}(\boldsymbol{\theta}) \mathbf{s}(t) + \mathbf{v}(t) \quad (4)$$

where  $\mathbf{a}(\theta_q) = [1, e^{j\frac{2\pi}{\lambda} d \sin \theta_q}, \dots, e^{j\frac{2\pi}{\lambda} (M-1) d \sin \theta_q}]^T$  is the array manifold vector,  $\mathbf{A}(\boldsymbol{\theta}) = [\mathbf{a}(\theta_1), \mathbf{a}(\theta_2), \dots, \mathbf{a}(\theta_Q)]^T$ ,  $\boldsymbol{\theta} = [\theta_1, \theta_2, \dots, \theta_Q]^T$  denotes the DOAs to be estimated and  $\theta_1 < \theta_2 < \dots < \theta_Q$ .  $\mathbf{v}(t) \sim \mathcal{CN}(\mathbf{0}, \sigma_v^2 \mathbf{I}_M)$  represents the additive white Gaussian noise (AWGN) vector.

Following the signal model (4), the received signal's covariance matrix can be expressed as

$$\mathbf{R} = \mathbf{A} \mathbf{R}_s \mathbf{A}^H + \sigma_v^2 \mathbf{I}_M = \sum_{q=1}^Q \sigma_{s_q}^2 \mathbf{a}(\theta_q) \mathbf{a}^H(\theta_q) + \sigma_v^2 \mathbf{I}_M \quad (5)$$

where  $\mathbf{A} = \mathbf{A}(\boldsymbol{\theta})$  and  $\mathbf{R}_s = \text{diag}\{\sigma_{s_1}^2, \dots, \sigma_{s_Q}^2\}$  denotes the signal power. However, since  $\mathbf{a}(\theta)$  is unknown, the signal covariance matrix cannot be obtained directly, the sample covariance matrix  $\hat{\mathbf{R}} = \frac{1}{T} \sum_{t=1}^T \mathbf{y}(t) \mathbf{y}^H(t)$  is considered as a substitution and if  $T \rightarrow \infty$ , we have the sample covariance  $\hat{\mathbf{R}}$  is equal to the statistical one  $\mathbf{R}$  in terms of the weak law of large number.

### 3. Tree-based DNN Model for High-Resolution DOA Estimation

In this section, a novel tree model-based DNN (TDNN) model is proposed for high-resolution DOA estimation and its detailed training procedure is described as well.

#### 3.1 Proposed Method

The proposed TDNN classifier is composed of  $H$  levels, and each level contains  $G_h$  fully-connected MLNNs, where  $1 \leq h \leq H$ . We let all the  $G_h$  networks in the same level of TDNN have identical structures, and their output layers all have  $L_h$  neurons. Then the sum output size of level  $h$  is  $G_h L_h$ , which is equal to the number of networks contained in level  $(h+1)$ , so  $G_{h+1}$  can be given by

$$G_{h+1} = G_h L_h = L_1 L_2 \cdots L_{h-1} L_h \quad (6)$$

for  $1 \leq h \leq H-1$  and  $G_1 = 1$ . As shown in Fig. 2, the feature vector  $\mathbf{r}$  is firstly input to  $\mathcal{D}_1$ , and the output layer of  $\mathcal{D}_1$  has  $L_1$  neurons. Then in order to join with the output size of level 1, level 2 contains  $L_1$  networks, i.e.,  $G_2 = L_1$ . So if a signal is divided into the class  $l_1$  by  $\mathcal{D}_1$ , where  $1 \leq l_1 \leq L_1$ , its corresponding feature vector  $\mathbf{r}$  will be then input to the  $l_1$ -th network of level 2 ( $\mathcal{D}_2^{l_1}$ ). After that,  $\mathcal{D}_2^{l_1}$  has  $L_2$  neurons in its output layer, and there are also  $L_2$  networks in level 3 connecting to it. Similarly, if the signal is labelled as class  $l_2$  by  $\mathcal{D}_2^{l_1}$ ,  $1 \leq l_2 \leq L_2$ ,  $\mathbf{r}$  will be input to  $\mathcal{D}_3^{l_1, l_2}$ . Therefore, when TDNN is used to perform DOA

estimation, only one network in each level will be activated. Thus the input feature vector is sequentially input to  $H$  networks, and by combining the classification results of these networks, we can obtain a  $H$ -dimensional numerical label vector  $\boldsymbol{\ell} = [l_1, l_2, \dots, l_H]^T$ , for  $1 \leq l_h \leq L_h$  and  $1 \leq h \leq H$ . According to  $\boldsymbol{\ell}$ , the decision procedure that  $\mathbf{r}$  experienced in TDNN can be summarized as

$$\mathbf{r} \longrightarrow \mathcal{D}_1 \xrightarrow{l_1} \mathcal{D}_2^{l_1} \xrightarrow{l_2} \dots \xrightarrow{l_{H-1}} \mathcal{D}_H^{l_1, l_2, \dots, l_{H-1}} \xrightarrow{l_H} \boldsymbol{\ell} \quad (7)$$

where the lower right symbol of  $\mathcal{D}$  denotes the level number, and the upper right symbols represent the accumulative labels of the previous levels.

Since TDNN is designed for solving DOA estimation problems, we firstly consider the single emitter case, i.e.,  $Q = 1$ , and assume the DOA  $\theta$  must fall in an angular interval  $\Theta = [\theta_{\min}, \theta_{\max})$ , i.e.  $\theta \in \Theta$ , and it is divided into  $L_1$  uniform sub-intervals by  $\mathcal{D}_1$  like  $\Theta = \bigcup_{l_1=1}^{L_1} \Theta_1^{l_1}$ , where  $\Theta_1^{l_1} = [\theta_{1,\min}^{l_1}, \theta_{1,\max}^{l_1})$ . Then  $\Theta_1^{l_1}$  can be further divided into smaller sub-intervals as  $\Theta_1^{l_1} = \bigcup_{l_2=1}^{L_2} \Theta_2^{l_1, l_2}$ , and  $\Theta = \bigcup_{l_1=1}^{L_1} \bigcup_{l_2=1}^{L_2} \Theta_2^{l_1, l_2}$ , where  $\Theta_2^{l_1, l_2} = [\theta_{2,\min}^{l_1, l_2}, \theta_{2,\max}^{l_1, l_2})$ . Therefore, level  $h$  of TDNN can divide  $\Theta$  into  $L_1 L_2 \cdots L_h$  uniform spatial subintervals, which is denoted by

$$\Theta = \bigcup_{l_1=1}^{L_1} \bigcup_{l_2=1}^{L_2} \dots \bigcup_{l_h=1}^{L_h} \Theta_h^{l_1, l_2, \dots, l_h} \quad (8)$$

where  $\Theta_h^{l_1, l_2, \dots, l_h} = [\theta_{h,\min}^{l_1, l_2, \dots, l_h}, \theta_{h,\max}^{l_1, l_2, \dots, l_h})$ . And we define the spatial resolution of level  $h$  as

$$\Delta\theta_h = \theta_{h,\max}^{l_1, l_2, \dots, l_h} - \theta_{h,\min}^{l_1, l_2, \dots, l_h} = \frac{\theta_{\max} - \theta_{\min}}{G_h L_h} \quad (9)$$

where  $\Delta\theta_1 > \Delta\theta_2 > \dots > \Delta\theta_H$ . Therefore, the size of subintervals divided by the last level, i.e.,  $\Delta\theta_H = \theta_{H,\max}^{l_1, l_2, \dots, l_H} - \theta_{H,\min}^{l_1, l_2, \dots, l_H}$ , represents the spatial resolution can be achieved by TDNN, which is expressed by

$$\Delta\theta = \Delta\theta_H = \frac{\theta_{\max} - \theta_{\min}}{G_H L_H} = \frac{\theta_{\max} - \theta_{\min}}{L_1 L_2 \cdots L_{H-1} L_H} \quad (10)$$

where we can get  $G_H = L_1 L_2 \cdots L_{H-1}$  based on (6). And the final estimated DOA  $\hat{\theta}$  is related to the classification labels of all the levels, which is given by

$$\hat{\theta} = \theta_{\min} + \boldsymbol{\ell}^T \Delta\boldsymbol{\theta} = \theta_{\min} + \sum_{h=1}^H l_h \Delta\theta_h \quad (11)$$

where  $\Delta\boldsymbol{\theta} = [\Delta\theta_1, \Delta\theta_2, \dots, \Delta\theta_H]^T$ . Equations (10) and (11) show the DOA estimation accuracy of the proposed TDNN classifier depends on the values of  $H$  and  $L_h$ .

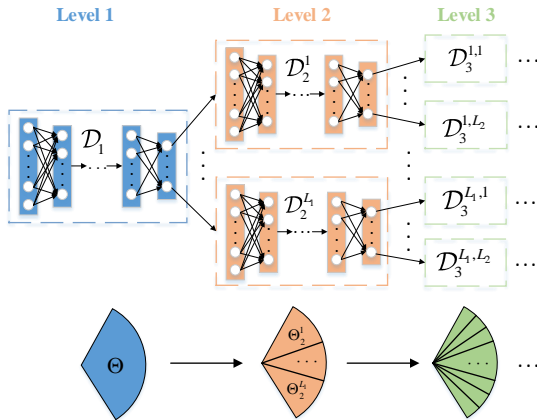


**Fig. 2.** The proposed TDNN contains  $H$  levels and each level has  $L_1 L_2 \cdots L_{h-1} L_h$  MLNNs, so the angle interval is also divided in to smaller sub-intervals with the increasing of TDNN's depth.

### 3.2 Training Procedure

All the MLNNs in the proposed TDNN classifier are feed forward networks and composed of three parts, one input layer, one output layer and some hidden layers. Since the networks in the same level has the same number of input and output neurons, in order to reduce the training burden, we let the networks in the same level have the identical network structure and we can train them in the parallel manner.  $\mathcal{D}_h$  represents an arbitrary network in the level  $h$  of TDNN, supposing it has  $K$  layers including one input layer, one output layer and  $K - 2$  hidden layers, then the computation steps of the  $k$ -th layer in  $\mathcal{D}_h$  are given by

$$\mathbf{q}_h^k = \mathbf{W}_h^{k,k-1} \mathbf{g}_h^{k-1} + \mathbf{b}_h^k, \quad \mathbf{g}_h^k = A[\mathbf{q}_h^k] \quad (12)$$

where  $1 \leq h \leq H, 1 \leq k \leq K$ .  $\mathbf{g}_h^k$  denotes the output vector in the  $k$ -th layer of  $\mathcal{D}_h$ , where  $\mathbf{g}_h^0 = \mathbf{r}$  and  $\mathbf{g}_h^K$  is the output of  $\mathcal{D}_h$ .  $\mathbf{W}_h^{k,k-1}$  represents the fully-connected weight matrix between the  $(k - 1)$ -th layer and  $k$ -th layer, and  $\mathbf{b}_h^k$  is the bias vector.  $A[\cdot]$  denotes the activation function, it is set as ReLU function for hidden layers, while Softmax function for output layer.

In order to reduce the instability caused by the uncertain signal waveforms, we choose the signal sample covariance matrix  $\mathbf{R}$  as the input feature for the proposed TDNN classifier. In addition, due to the unknown noise variance and the lower left elements of  $\mathbf{R}$  are conjugate replicas of the upper right ones, then delete the redundant elements in  $\mathbf{R}$  and the final input vector is reformulated by the off-diagonal upper right elements of  $\mathbf{R}$ , given by

$$\mathbf{r} = [\text{Re}(\bar{\mathbf{r}}^T), \text{Im}(\bar{\mathbf{r}}^T)]^T \in \mathbb{R}^{M(M-1) \times 1} \quad (13)$$

where  $\bar{\mathbf{r}} = [R_{1,2}, \dots, R_{1,M}, R_{2,3}, \dots, R_{M-1,M}]^T \in \mathbb{C}^{M(M-1)/2 \times 1}$  and  $R_{i,j}$  denotes the  $(i, j)$ -th element of  $\mathbf{R}$ . In the prediction period, since the covariance matrix is unavailable, the testset consists of the off-diagonal upper right elements of the sample covariance matrix  $\bar{\mathbf{R}}$ .

Since MLNNs in level  $h$  have same structures, let  $\mathbf{z}^h$  represent the one-hot form label vector for training  $\mathcal{D}_h$ , which is an  $L_h \times 1$  binary vector with  $\|\mathbf{z}^h\| = 1$  and its relationship with  $\ell$  can be expressed as

$$\mathbf{z}^h(\ell(h)) = \mathbf{z}^h(l_h) = 1. \quad (14)$$

Therefore, by combining the training data and training label, the complete training set for the  $i$ -th MLNN is given as  $\mathbb{T} = \{(\mathbf{r}, \mathbf{z}^h)\}$ . Then we define  $\hat{\mathbf{z}}^h$  as the output prediction vector of  $\mathcal{D}_h$  for  $\mathbf{r}$ , which is in the form of probability distribution. So we choose binary cross entropy (BCE) as the loss function and it is given as

$$\text{loss} = -\frac{1}{L_h} \sum_{l_h=1}^{L_h} \left[ \mathbf{z}^h(l_h) \log(\hat{\mathbf{z}}^h(l_h)) + (1 - \mathbf{z}^h(l_h)) \log(1 - \hat{\mathbf{z}}^h(l_h)) \right]. \quad (15)$$

Then the optimal weights and biases of  $\mathcal{D}_h$  can be obtained by minimizing this loss function.

### 3.3 Complexity Analysis

In the prediction stage, only one MLNN in each level of TDNN is activated for per DOA estimation, then the complexity of TDNN comes from two parts, i.e., model complexity and computation complexity. Firstly, we define the model complexity as the number of output classes required for achieving a specific resolution  $\Delta\theta$ , so the model complexity of conventional DNN is  $\mathcal{M}(\text{DNN}) = \mathcal{O}(N)$ , where  $N = (\theta_{\max} - \theta_{\min}) / \Delta\theta$ . Then the model complexity of TDNN is given by

$$\mathcal{M}(\text{TDNN}) = \mathcal{O}\left(\sum_{h=1}^H L_h\right), \quad (16)$$

from (10) we know  $N = L_1 L_2 \cdots L_H$ , so it is obvious that  $\mathcal{M}(\text{TDNN}) \ll \mathcal{M}(\text{DNN})$ .

As discussed in [11], the computation complexity of a network is proportional to the number of layers and the number of neurons in each layer. So as the summation of all the activated MLNNs, the computation complexity of TDNN is

$$C(\text{TDNN}) = \mathcal{O}\left(\sum_{h=1}^H \sum_{k=1}^{K-1} W_h^k W_h^{k+1}\right) \quad (17)$$

where  $W_h^k$  denotes the number of neurons contained in the  $K$ -th layer of  $\mathcal{D}_h$ . And the comparison with the computation complexity of conventional DNN models will be displayed in simulation section.

## 4. Extensive TDNN-based Method for Multi-Emitter Scenarios

As the number of signal sources increases, the corresponding DOA estimation problem is converted into a multi-label learning problem. For conventional DNN-based DOA

estimation algorithms, each unit in the output layer corresponds to an independent angle, so when the combined signals from  $Q$  different sources are input to the DNN, the training label vector will be a binary vector  $\mathbf{z}_{\text{DNN}}$  which contains  $Q$  '1' elements, i.e.,  $\|\mathbf{z}_{\text{DNN}}\|_1 = Q$ . However, for our proposed TDNN, since the output neurons of each level correspond to different angular regions, it is possible that several DOAs in the same region under the multi-emitter case, then there will appear that different signals marked by same label and thus the binary vector cannot express it. Therefore, we give an  $L_h \times Q$  binary label matrix for classifying the  $Q$ -emitters signals input to  $\mathcal{D}_h$

$$\mathbf{Z}^h = \begin{bmatrix} \mathbf{z}_1^h & \mathbf{z}_2^h & \cdots & \mathbf{z}_Q^h \end{bmatrix} \quad (18)$$

where  $\mathbf{z}_q^h$  denotes the one-hot form label vector of the  $q$ -th signal and  $\|\mathbf{z}_q^h\|_1 = 1$ .

Since the feature vector  $\mathbf{r}$  is only constructed by the upper right elements of  $\mathbf{R}$  and has no connection with noise, then by observing (5) that  $\mathbf{r}$  can be separated into  $Q$  components under  $Q$ -sources cases as

$$\mathbf{r} = \mathbf{r}_1 + \mathbf{r}_2 + \cdots + \mathbf{r}_Q \quad (19)$$

where  $\mathbf{r}_q$  is the feature component of  $\theta_q$  and its elements are from the upper right part of  $\sigma_{s_q}^2 \mathbf{a}(\theta_q) \mathbf{a}^H(\theta_q)$ . Therefore, by drawing on the idea of binary relevance, we consider transforming the  $Q$ -emitters DOA estimation problem into  $Q$  single-source problems. And when solving the  $q$ -th problem, we can regard  $\mathbf{r}_q$  as the principal component and  $\mathbf{r}$  is classified as  $\theta_q$ . Then the  $Q$ -TDNN algorithm is proposed based on this principle.

As shown in Fig. 3,  $Q$ -TDNN is composed of  $Q$  TDNNs with same structures, and TDNN  $q$  is used to solve the  $q$ -th problem. Firstly,  $\mathbf{r}$  is separately input to these  $Q$  TDNNs,  $\boldsymbol{\ell}_q = [l_{q,1}, l_{q,2}, \cdots, l_{q,H}]^T$  denotes classification result of TDNN  $q$ , then we can obtain the estimation result of  $\theta_q$  as

$$\hat{\theta}_q = \theta_{\min} + \boldsymbol{\ell}_q^T \Delta \boldsymbol{\theta} = \theta_{\min} + \sum_{h=1}^H l_{q,h} \Delta \theta_h, \quad (20)$$

then by combining all the  $Q$  results, the complete DOA estimation result of  $Q$ -TDNN is given as  $\hat{\boldsymbol{\theta}}_{Q\text{-TDNN}} = [\hat{\theta}_1, \hat{\theta}_2, \cdots, \hat{\theta}_Q]$ .

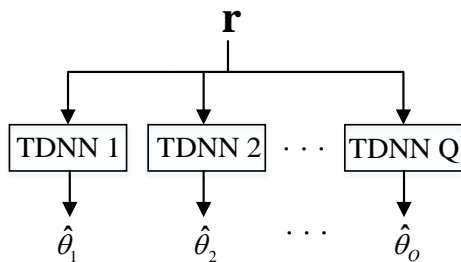


Fig. 3. Proposed  $Q$ -TDNN for multi-emitter DOA estimation.

Since the  $Q$ -TDNN contains  $Q$  TDNNs, and they have the same architectures, then the computation complexity of  $Q$ -TDNN is given by

$$C(Q\text{-TDNN}) = Q \cdot C(\text{TDNN}). \quad (21)$$

Then in the training duration, the training strategy for each TDNN is basically same as that for basic TDNN, let  $\mathbf{z}_q^h$  denote the training label vector of  $\mathbf{r}$  in  $\mathcal{D}_{q,h}$  which is an arbitrary DNN in the  $h$ -th layer of TDNN  $q$ , and  $\mathbf{z}_q^h(l_{q,h}) = 1$ . In addition, to increase the flexibility of the algorithm so that it is not limited to just  $Q$ -emitters case, we can add the signals of  $Q'$ -emitters into the training set, where  $Q' \leq Q$ , then when a  $Q'$ -emitters signal need to be estimated, we can just activate the first  $Q'$  TDNN classifiers of  $Q$ -TDNN. In this way, the proposed method can handle the scenario that the number of emitters is variable, and it makes  $Q$ -TDNN more practical than ML-DNN.

## 5. Simulation Results

In this section, the DOA estimation performance of the proposed methods is verified by performing a series of numerical simulations. The receive array is equipped with a 64-elements ULA, the DOAs of all the signals are fall in the angular region  $\Theta = [-60^\circ, 60^\circ]$ . These simulations were all completed on a desktop computer with Windows 10, AMD Ryzen 7 5800X CPU and NVIDIA GeForce RTX 4070Ti GPU. The software environment setup comprises Python 3.9 and Tensorflow 2.6.0. The angular range is uniformed sampled with interval  $1^\circ$ , the considered SNR range is  $[-20 \text{ dB}, 10 \text{ dB}]$  and SNR sample interval is 5 dB, and each sample is randomized 50 times, so the size of training dataset is  $N_t = 50N_\theta N_{\text{SNR}}$ . The validation dataset is 10% part of training dataset. The test dataset is constructed based on the same principle as training dataset with the number of randomization is 1000. Adam [20] is employed as optimizer, the learning rate is 0.005, the number of batch size and epochs are set as 1000 and 150<sup>1</sup>. The proposed TDNN method is mainly compared to DNN and root-MUSIC, where the fully-connected DNN considered in this work is a widely used DL model in the DOA estimation [18], regression DNN [21] and root-MUSIC is a classical subspace-based off-grid DOA estimation algorithm [22].

Table 1 lists the model parameters of the proposed TDNN, where  $H$  denotes the depth of TDNN and  $G_h$  represents the number of DNNs contained in each level. The specific network structures of the DNNs are also shown in this table. The selection of these model parameters is depend on complexity and the requirement of DOA estimation resolution. Increasing the depth  $H$  or the number of MLNNs in each level can improve the resolution, but also adds the complexity, so we have to make a balance between resolution and complexity when design a TDNN.

<sup>1</sup>The source code of this paper is available on request, readers can contact authors for it.

	$H$	$G_h$	Input layer	Hidden layers	Output layer
2-level TDNN	2	1/12	4032	512, 256, 128, 64, 32, 16	12/10
3-level TDNN	3	1/6/30	4032	512, 256, 128, 64, 32, 16	6/5/4

Tab. 1. Model parameters of the proposed TDNN.

Figure 4 plots the training performance versus the model complexity of DNNs. From this figure, it is seen that the model accuracy of DNNs becomes worse with the increasing of output classes. This means small-scale networks can have better model accuracy than large-scale networks. The specific impact on DOA estimation performance will be analyzed in the following by combining Fig. 5.

Figure 5 demonstrates the DOA RMSE versus SNR of the proposed TDNN with DNN, root-MUSIC and CRLB. The specific parameters involved in this simulation are as follows: the number of snapshots  $T = 50$ ,  $Q = 1$  and  $\theta = 27^\circ$ . From this figure, it can be seen that TDNN attains obvious performance gains over conventional DNN and root-MUSIC at  $\text{SNR} \leq -5\text{ dB}$ . TDNN can also nearly achieve CRLB at  $\text{SNR} = -10\text{ dB}$ , while DNN can only achieve it at  $\text{SNR} = 0\text{ dB}$ . The proposed TDNNs also have significantly performance advantages over regression DNN as  $\text{SNR} \leq -10\text{ dB}$ , which has higher resolution than DNNs designed based on classification principle. Additionally, the comparison between TDNNs with different structures is noteworthy. The performance of 3-level TDNN is better than 2-level TDNN, and from Tab. 1 we can find the model complexity of 3-level TDNN is also lower than 2-level TDNN. Therefore, by combining the conclusion of Fig. 4, we can conclude lower model complexity makes higher DOA estimation accuracy, and it is a key index must be considered when a TDNN model is constructed.

In order to evaluate the performance of the proposed method across the entire test set, Figure 6 plots the RMSE values of TDNN and root-MUSIC at different angular positions within  $[-60^\circ, 60^\circ]$ , where  $\text{SNR} = -10\text{ dB}$  and  $T = 50$ . From this figure we can see, the proposed TDNNs achieve significantly advantages over traditional method at all the angular positions. And similar to the conclusion obtained from Fig. 5, 3-level TDNN also has better performance than 2-level TDNN at most angular positions. So the proposed TDNN has guaranteed DOA estimation performance at entire angular region.

Figure 7 depicts the DOA estimation RMSE versus of  $Q$ -TDNN, DNN and root-MUSIC under the multi-emitter scenarios and  $\text{SNR} = -8\text{ dB}$ , and the DOAs are selected from set  $\{-15^\circ, -5^\circ, 5^\circ, 15^\circ, 25^\circ\}$ . It can be seen from this figure the RMSE of these three methods are very close when  $Q = 1$ , but as the number of emitters increases, the performance gap between the other two methods and TDNN is increasing, when  $Q = 5$ ,  $Q$ -TDNN has about  $16^\circ$  performance advantage over root-MUSIC and  $8.5^\circ$  over DNN. Therefore, the proposed  $Q$ -TDNN is confirmed to be a much more accurate method for the multi-emitter cases.

Finally, Figure 8 shows the computation complexity of TDNNs and DNN. TDNN is equivalent to  $Q$ -TDNN as  $Q \geq 2$ . Since the structure of conventional DNN keeps invariant with the increases of  $Q$ , its computation complexity is also fixed. As TDNN only activates one network in each level for per DOA estimation, the computation complexity of TDNN is significantly lower than that of DNN with any structures. The computation speeds of TDNNs and DNN are also given in Tab. 2, it's obviously that the proposed TDNN, whether it is 2-level or 3-level, takes much less time than DNN to perform a DOA estimation, and the difference is more than 2 seconds. Then combining all the simulation results, it can be concluded that TDNN is a much better model than conventional DNN because it can achieve significantly higher accuracy with much lower computation complexity.

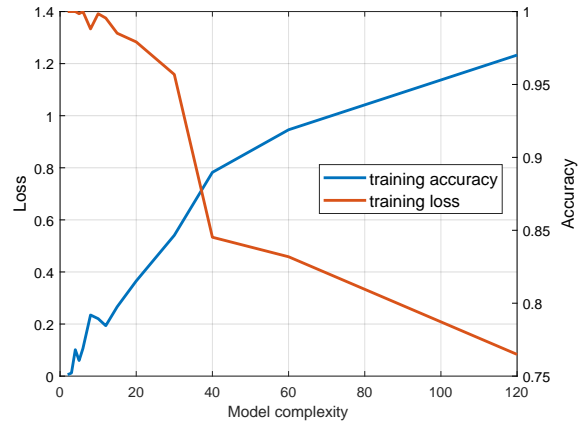


Fig. 4. Relationship between training performance and model complexity of DNN.

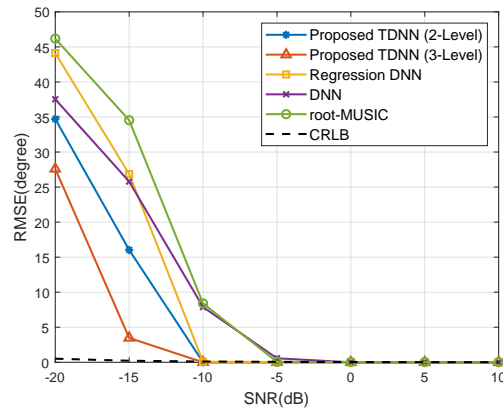


Fig. 5. RMSE versus SNR.

	2-level TDNN	3-level TDNN	DNN
Time [s]	1.35	1.87	3.86

Tab. 2. Computation time per DOA estimation.

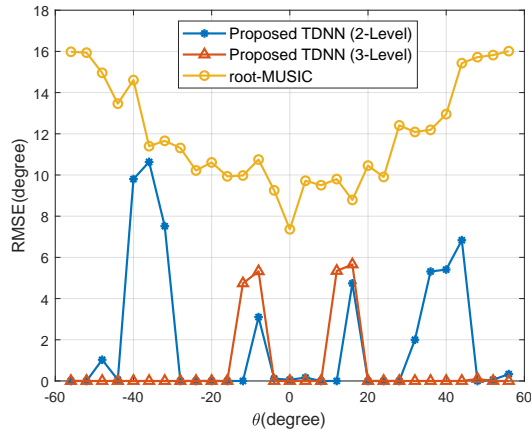


Fig. 6. RMSE versus different DOAs.

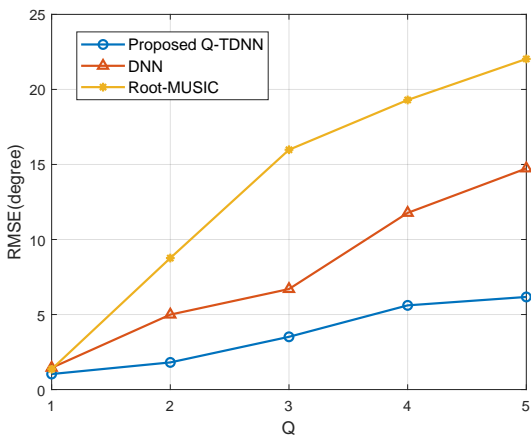


Fig. 7. RMSE versus the number of emitters.

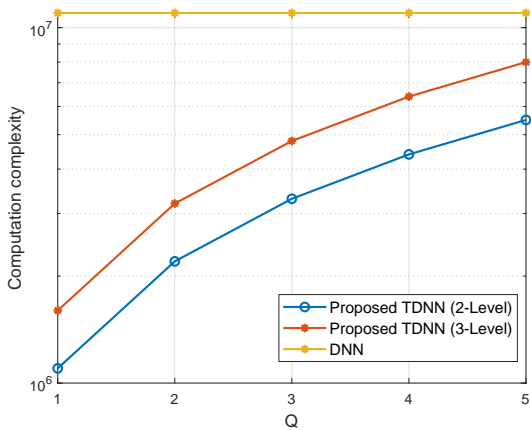


Fig. 8. Computation complexity versus the number of emitters.

## 6. Conclusions

In this work, a novel multi-level tree-based DNN model for high-resolution DOA estimation with massive MIMO receive array was proposed. Each level of TDNN adopts small-scale MLNNs as nodes to partition the target angular interval into multiple sub-intervals and each output class is associated to a MLNN at the next level. As the number of MLNNs increases from the first level to the last level, and so as the sum output classes. Therefore, TDNN can improve the DOA

estimation accuracy by adding the number of levels without increasing the model complexity of each MLNN. The proposed TDNN performs much better than conventional methods like Root-MUSIC, DNN when SNR is in the extremely low region ( $< -5$  dB). Additionally,  $Q$ -TDNN method is also designed for multi-emitter scenarios on basis of TDNN. The performance enhancement of  $Q$ -TDNN over DNN and root-MUSIC also increases as the number of emitters increases. In the future, we will continue to explore the applications of deep learning in areas such as sensing, positioning, and expand the research scenarios to wideband, near-field, etc.

## Acknowledgments

This work was supported in part by the National Key Research and Development Program of China (2022YFE0122300), in part by the National Natural Science Foundation of China (Nos. U22A2002, 62171217 and 62071234), the Hainan Province Science and Technology Special Fund (ZDKJ2021022), the Scientific Research Fund Project of Hainan University under Grant KYQD(ZR)-21008, and the Collaborative Innovation Center of Information Technology, Hainan University (XTCX2022XXC07).

## References

- [1] HEATH, R. W., GONZALEZ-PRELCIC, N., RANGAN, S., et al. An overview of signal processing techniques for millimeter wave MIMO systems. *IEEE Journal of Selected Topics in Signal Processing*, 2016, vol. 10, no. 3, p. 436–453. DOI: 10.1109/JSTSP.2016.2523924
- [2] XU, L., WEN, F., ZHANG, X., et al. A novel unitary PARAFAC algorithm for joint DOA and frequency estimation. *IEEE Communications Letters*, 2019, vol. 23, no. 4, p. 660–663. DOI: 10.1109/LCOMM.2019.2896593
- [3] CHEN, P., YANG, Z., CHEN, Z., et al. Reconfigurable intelligent surface aided sparse DOA estimation method with non-ULA. *IEEE Signal Processing Letters*, 2021, vol. 28, p. 2023–2027. DOI: 10.1109/LSP.2021.3116789
- [4] ZHANG, R., XIA, W., YAN, F., et al. A single-site positioning method based on TOA and DOA estimation using virtual stations in NLOS environment. *China Communications*, 2019, vol. 16, no. 2, p. 146–159. DOI: 10.12676/j.cc.2019.02.010
- [5] CHENG, L., WU, Y., ZHANG, J., et al. Subspace identification for DOA estimation in massive/full-dimension MIMO systems: Bad data mitigation and automatic source enumeration. *IEEE Transactions on Signal Processing*, 2015, vol. 63, no. 22, p. 5897–5909. DOI: 10.1109/TSP.2015.2458788
- [6] LI, B., ZHANG, X., LI, J., et al. DOA estimation of non-circular source for large uniform linear array with a single snapshot: Extended DFT method. *IEEE Communications Letters*, 2021, vol. 25, no. 12, p. 3843–3847. DOI: 10.1109/LCOMM.2021.3120211
- [7] WEN, F., CUI, G., GACANIN, H., et al. Compressive sampling framework for 2D-DOA and polarization estimation in mmwave polarized massive MIMO systems. *IEEE Transactions on Wireless Communications*, 2023, vol. 22, no. 5, p. 3071–3083. DOI: 10.1109/TWC.2022.3215965

- [8] SHU, F., QIN, Y., LIU, T., et al. Low-complexity and high-resolution DOA estimation for hybrid analog and digital massive MIMO receive array. *IEEE Transactions on Communications*, 2018, vol. 66, no. 6, p. 2487–2501. DOI: 10.1109/TCOMM.2018.2805803
- [9] LI, S., LIU, Y., YOU, L., et al. Covariance matrix reconstruction for DOA estimation in hybrid massive MIMO systems. *IEEE Wireless Communications Letters*, 2021, vol. 9, no. 8, p. 1196–1200. DOI: 10.1109/LWC.2020.2985014
- [10] HUANG, H., YANG, J., HUANG, H., et al. Deep learning for super-resolution channel estimation and DOA estimation based massive MIMO system. *IEEE Transactions on Vehicular Technology*, 2018, vol. 67, no. 9, p. 8549–8560. DOI: 10.1109/TVT.2018.2851783
- [11] HU, D., ZHANG, Y., HE, L., et al. Low-complexity deep-learning-based DOA estimation for hybrid massive MIMO systems with uniform circular arrays. *IEEE Wireless Communications Letters*, 2020, vol. 9, no. 1, p. 83–86. DOI: 10.1109/LWC.2019.2942595
- [12] PAPAGEORGIOU, G. K., SELLATHURAI, M., ELDAR, Y. C., et al. Deep networks for direction-of-arrival estimation in low SNR. *IEEE Transactions on Signal Processing*, 2021, vol. 69, p. 3714–3729. DOI: 10.1109/TSP.2021.3089927
- [13] WU, L., LIU, Z., HUANG, Z. Deep convolution network for direction of arrival estimation with sparse prior. *IEEE Signal Processing Letters*, 2019, vol. 26, no. 11, p. 1688–1692. DOI: 10.1109/LSP.2019.2945115
- [14] CONG, J., WANG, X., YAN, C., et al. CRB weighted source localization method based on deep neural networks in multi-UAV network. *IEEE Internet of Things Journal*, 2023, vol. 10, no. 7, p. 5747–5759. DOI: 10.1109/JIOT.2022.3150794
- [15] YU, J., WANG, Y. Deep learning-based multipath DoAs estimation method for mmWave massive MIMO systems in low SNR. *IEEE Transactions on Vehicular Technology*, 2023, vol. 72, no. 6, p. 7480–7490. DOI: 10.1109/TVT.2023.3239402
- [16] WU, X., YANG, X., JIA, X., et al. A gridless DOA estimation method based on convolutional neural network with Toeplitz prior. *IEEE Signal Processing Letters*, 2022, vol. 29, p. 1247–1251. DOI: 10.1109/LSP.2022.3176211
- [17] ZHANG, M., ZHOU, Z. A review on multi-label learning algorithms. *IEEE Transactions on Knowledge and Data Engineering*, 2014, vol. 26, no. 8, p. 1819–1837. DOI: 10.1109/TKDE.2013.39
- [18] XU, S., BRIGHENTE, A., CHEN, B., et al. Deep neural networks for direction of arrival estimation of multiple targets with sparse prior for line-of-sight scenarios. *IEEE Transactions on Vehicular Technology*, 2023, vol. 72, no. 4, p. 4683–4696. DOI: 10.1109/TVT.2022.3224586
- [19] ZHAN, X., SUN, Z., SHU, F., et al. Rapid phase ambiguity elimination methods for DOA estimator via hybrid massive MIMO receive array. *Chinese Journal of Electronics*, 2024, vol. 33, no. 1, p. 175–184. DOI: 10.23919/cje.2022.00.112
- [20] KINGMA, D. P., BA, J. Adam: a method for stochastic optimization. *arXiv*, 2014, arXiv:1412.6980, p. 1–15. DOI: 10.48550/arXiv.1412.6980
- [21] CHEN, M., MAO, X., WANG, X. Performance analysis of deep neural networks for direction of arrival estimation of multiple sources. *IET Signal Processing*, 2023, vol. 17, no. 3, p. 1–18. DOI: 10.1049/sil2.12178
- [22] BARABELL, A. Improving the resolution performance of eigenstructure-based direction-finding algorithms. In *IEEE International Conference on Acoustics, Speech, and Signal Processing (ICASSP)*. Boston (MA, USA), 1983, vol. 8, p. 336–339. DOI: 10.1109/ICASSP.1983.1172124

## About the Authors ...

**Yifan LI** was born in 1997. He received his B.Sc. from North University of China, Taiyuan, China, in 2019. He is currently pursuing the Ph.D. degree with the School of Electronic and Optical Engineering, Nanjing University of Science and Technology, Nanjing, China. His research interests include array signal processing, massive MIMO system, and machine-learning.

**Feng SHU** (corresponding author) received the B.S. degree from Fuyang Teaching College, Fuyang, China, in 1994, the M.S. degree from Xidian University, Xian, China, in 1997, and the Ph.D. degree from Southeast University, Nanjing, China, in 2002. From September 2009 to September 2010, he was a Visiting Postdoctoral Fellow with the University of Texas at Dallas, Richardson, TX, USA. From July 2007 to September 2007, he was a Visiting Scholar with the Royal Melbourne Institute of Technology (RMIT University), Melbourne, VIC, Australia. From October 2005 to November 2020, he was with the School of Electronic and Optical Engineering, Nanjing University of Science and Technology, Nanjing, where he was promoted from an Associate Professor to a Full Professor of supervising Ph.D. students in 2013. Since December 2020, he has been with the School of Information and Communication Engineering, Hainan University, Haikou, China, where he is currently a Professor and a supervisor of Ph.D. and graduate students. His research interests include machine learning, security, location, and DOA measurement in wireless networks.

**Yaoliang SONG** was born in Wuxi, China, in 1960. He received the B.Eng., M.Eng., and Ph.D. degrees in Electrical Engineering from the Nanjing University of Science and Technology, China, in 1983, 1986, and 2000, respectively. From 2004 to 2005, he was a Research Fellow with the Department of Engineering Science, University of Oxford. He is currently a Professor with the Nanjing University of Science and Technology, where he is also the Head of the UWB Radar Imaging Group. His research interests include UWB communication, UWB radar imaging, and advanced signal processing.

**Jiangzhou WANG** has been a Professor with the University of Kent, U.K., since 2005. He has published over 400 papers and four books in the areas of wireless communications. He was a recipient of the Best Paper Award from the IEEE GLOBECOM 2012. He was an IEEE Distinguished Lecturer from 2013 to 2014. He was the Technical Program Chair of the 2019 IEEE International Conference on Communications, Shanghai, the Executive Chair of the IEEE ICC 2015, London, and the Technical Program Chair of the IEEE WCNC 2013. He has served as an Editor for a number of international journals, including IEEE Transactions on Communications from 1998 to 2013. He is a Fellow of the Royal Academy of Engineering, U.K., and IET.